



OPEN

Green synthesis of bimetallic ZnO–CuO nanoparticles and their cytotoxicity properties

Yan Cao¹, Hayder A. Dhahad², M. A. El-Shorbagy^{3,4}, Hajar O. Alijani⁵, Mana Zakeri⁶, Abolfazl Heydari⁷, Ehsan Bahonar⁸, Miroslav Slouf⁹, Mehrdad Khatami¹⁰✉, Mahin Naderifar¹¹, Siavash Irvani¹², Sanaz Khatami¹³ & Farnaz Farzaneh Dehkordi¹⁴✉

In this study, a simple and green strategy was reported to prepare bimetallic nanoparticles (NPs) by the combination of zinc oxide (ZnO) and copper oxide (CuO) using *Sambucus nigra* L. extract. The physicochemical properties of these NPs such as crystal structure, size, and morphology were studied by X-ray diffraction (XRD), field emission gun scanning electron microscopy (FEG-SEM), and transmission electron microscopy (TEM). The results suggested that these NPs contained polyagonal ZnO NPs with hexagonal phase and spherical CuO NPs with monoclinic phase. The anticancer activity of the prepared bimetallic NPs was evaluated against lung and human melanoma cell lines based on MTT assay. As a result, the bimetallic ZnO/CuO NPs exhibited high toxicity on melanoma cancer cells while their toxicity on lung cancer cells was low.

Cancer can cause the unregulated cell growth with high potential to invade and spread to other cells and tissues of the body by the lymph system and blood via a metastatic process^{1,2}. Cancer as one of the most aggressive diseases kills more than ten million people every year³. Lung cancer and melanoma are the most deadly ones. One of the most important features of the cancer cells compared to somatic cells is their ability to replicate and spread to different parts of the body. Cancer cells release a variety of factors into their environment which can change the function of cells in the tumor microenvironment⁴. One of the reasons for the high mortality rate of patients with lung cancer and melanoma is the uncontrolled growth of cancer cells in the lung and skin tissue, metastasis and spread to sensitive organs (such as the brain). Currently, the most common treatments for cancer are surgery, radiation therapy, immunotherapy, hormonal therapy, and chemotherapy⁵, but recently many researchers have turned to nanomaterials and herbal anticancer drugs^{6,7}. Despite some advantages, conventional chemotherapy is discouraging to invest more in drug discovery and/or drug delivery systems due to some drawbacks such as poor bioavailability of drugs to tumor tissues, adverse side effects, low therapeutic indices, high dose requirements, non-specific targeting, and multidrug resistance^{8,9}. Different evaluations have been performed on the anticancer properties of various nanoscaled structures, composites, RNAs, and polymers^{10–23}.

The biomedical potentials of various secondary metabolites such as phenolic compounds, flavonoids, glycosides, terpenoids and aldehydes have been evaluated^{24–26}. Therapeutic methods based on the application of encapsulated herbal compounds in nanomaterials²⁷, hyperthermia, targeted delivery of genes or anticancer drugs to the cells/tissues have resulted in efficient cell death of cancer cells in the targets²⁸. Indeed, rapid proliferation of cancer cells and necrosis of normal cells in the body are prominent features of cancer cells and

¹School of Mechatronic Engineering, Xi'an Technological University, Xi'an 710021, China. ²Mechanical Engineering Department, University of Technology, Baghdad, Iraq. ³Department of Mathematics, College of Science and Humanities in Al-Kharj, Prince Sattam Bin Abdulaziz University, Al-Kharj 11942, Saudi Arabia. ⁴Department of Basic Engineering Science, Faculty of Engineering, Menoufia University, Shebin El-Kom 32511, Egypt. ⁵Department of Biotechnology, Shahid Bahonar University of Kerman, Kerman, Iran. ⁶Department of Biology, Islamic Azad University, Tehran Medical Branch, Tehran, Iran. ⁷Polymer Institute of the Slovak Academy of Sciences, Dúbravská Cesta 9, 845 41 Bratislava, Slovakia. ⁸Faculty of Chemical and Petroleum Engineering, Sahand University of Technology, Tabriz, Iran. ⁹Institute of Macromolecular Chemistry, Czech Academy of Sciences, Heyrovskeho nam. 2, 162 06 Prague 6, Czech Republic. ¹⁰Noncommunicable Diseases Research Center, Bam University of Medical Sciences, Bam, Iran. ¹¹Faculty of Nursing & Midwifery, Zabol University of Medical Sciences, Zabol, Iran. ¹²Faculty of Pharmacy and Pharmaceutical Sciences, Isfahan University of Medical Sciences, Isfahan, Iran. ¹³Department of Medical Biotechnology, School of Advanced Technologies in Medicine, Shahid Beheshti University of Medical Sciences, Tehran, Iran. ¹⁴Department of Biology, Ardabil Branch, Islamic Azad University, Ardabil, Iran. ✉email: mehrdad7khatami@gmail.com; Farzaneh_farnaz2007@yahoo.com

side effects of current cancer therapy. Rapid and targeted penetration in cancer cells can prevent the spread of disease to other tissues, and thus control the cancer. Nanoparticles (NPs) have gained interest of scientists in the field of nanomedicine^{29–36}. The therapeutic effects of NPs depend on the particle size, the culture time of the target cell, the amount of metal in the targeted cell, and their physicochemical properties^{36–39}. On the other hand, bimetallic and multimetallic NPs have shown unique physicochemical properties with synergistic effects and high functionality⁴⁰. These integrated NPs have more reactive sites, increased efficiency, and greater stability^{41,42}. In recent decades, the antitumor activity of different biogenic and non-biogenic bimetallic NPs has been evaluated^{43–45}. In 2019, Lomelí-Marroquín et al. synthesized silver/gold bimetallic NPs with the aim of reducing the nano metallic toxicity of silver, and evaluated their antitumor activity on melanoma cancer cells⁴⁶. Pt/Pd bimetallic NPs were synthesized using *Dioscorea bulbifera* extract, and gold-silver bimetallic NPs were synthesized using *Stigmaphyllon ovatum* leaf extract; their anticancer activity against HeLa cells was also investigated^{47,48}. In another study, the gold(i)-BODIPY-imidazole bimetallic complex demonstrated good anti-proliferative activity against breast, colon, and prostate cancer⁴⁹. In 2019, silver/palladium bimetallic NPs were synthesized using *Terminalia chebula* fruit extract, and their antitumor properties were evaluated against A549⁵⁰. Additionally, biogenic copper and zinc oxide NPs were synthesized in 2018 and 2019, and their anticancer activities were evaluated against T98G human glomerular superficial cell and cervical cancer, respectively^{51,52}. Typically, the synthesis of multimetallic and bimetallic NPs is costly and time-consuming, and may include toxic or hazardous substances. Metal oxide NPs such as zinc oxide (ZnO) and copper oxide (CuO) demonstrated diverse biological applications; these NPs were highly compatible with normal cells in the body. Biogenic ZnO NPs were eco-friendly synthesized using *Cardiospermum halicacabum* and *Mangifera indica* leaf extracts, and they illustrated good antitumor properties against A375 and A549 cells at a concentration of 50 µg/mL, respectively^{4,53}. In another study, CuO NPs were synthesized using a green method; these NPs inhibited mRNAII expression in A549 cancer cells and stimulated apoptosis⁵⁴. In 2017, Chakraborty et al. reported an IC₅₀ (the concentration of NPs caused 50% mortality) of 1.71 µg/mL for CuO NPs against A375 cancer cells⁵⁵.

ZnO and CuO NPs can be applied in cancer therapy, cosmetic creams, and industrial catalysts. ZnO NPs are widely employed due to the production of reactive oxygen species (ROS) and their unique electrostatic behavior, which can prevent DNA damage. At physiological pH, ZnO NPs find a positive charge that increases the body's phagocytic activity and the death of cancer cells⁵⁶. In one study, Ahamed et al. showed that CuO NPs had the genotoxic toxicity on A549 cells. These metallic NPs caused apoptosis via lipid peroxidation and oxidative stress in lung cancer cells. But, Cu ions released from the surface of CuO NPs have insufficient toxicity against the other cancer cells⁵⁷. In 2020, Duan et al. proved that green-synthesized ZnO NPs could induce the apoptosis in A375 cancer cells by increasing the amount of ROS⁴. Besides, Dobrucka et al. showed that green-fabricated bimetallic ZnO/CuO NPs could stop the cell division and cell death in T98G cancer cells by inhibiting the cell cycle in the G2-M stage. In another study, Elemike et al. demonstrated that bimetallic ZnO/CuO synthesized by low cost and green method had less anticancer effects on Hela cancer cells than the control drug 5-fluorouracil⁵². Green synthesis of bimetallic ZnO/CuO using *Sambucus nigra* L. plant extract was illustrated, with the advantages of simplicity, cost-effectiveness, low temperature, eco-friendliness, desirable anticancer properties, and efficient cytotoxicity of biogenic ZnO/CuO NPs⁵¹. Using synergistic biological effects such as increased ROS production, Cu genotoxicity, and increased cancer cell apoptosis, these materials can be employed as effective therapeutic agents in the treatment of lung and melanoma cancer.

The medicinal plant black elderberry with the scientific name of *Sambucus nigra* L. from the Caprifoliaceae family was collected from the forest of Mazandaran, Iran. This plant contains different types of secondary metabolites including glycosidic compounds, terpenoids, phenolics, tannins, anthocyanins, etc. In traditional medicine, *S. nigra* was utilized to treat bone fractures, kidney diseases, respiratory diseases, and eczema⁵⁸. Generally, green and eco-friendly synthetic strategies are deployed instead of conventional industrial manufacturing methods to eliminate/prevent hazardous materials and reduce expensive/complex instruments and materials. These eco-friendly methods have some benefits compared to the conventional physicochemical approaches such as simplicity, rapidness, cost-effectiveness, low toxicity, and environmentally friendliness. In this study, bimetallic ZnO/CuO NPs have been synthesized using *S. nigra* L. extract via a green and simple method. The synthesized bimetallic NPs have been characterized by X-ray diffraction (XRD), field emission gun scanning electron microscopy (FEG-SEM), and transmission electron microscopy (TEM) combined with energy dispersive analysis of X-rays (EDX) and selected area electron diffraction (SAED). Additionally, the anticancer activity of these NPs have been evaluated on human melanoma cell line (A375) and human lung cancer (A549).

Materials and methods

Materials. Dulbecco's Modified Eagle's Medium (DMEM; GIBCO), antibiotics like penicillin (GIBCO), and streptomycin (GIBCO) were purchased from Invitrogen, U.K. Fetal Calf Serum (FCS; GIBCO), glutamine (GIBCO), and sodium pyruvate (GIBCO) were purchased from Invitrogen USA. Acetic acid, zinc (II) acetate ($\text{Zn}(\text{CH}_3\text{COO})_2 \cdot 2\text{H}_2\text{O} \leq 100\%$), copper (II) chloride ($\text{CuCl}_2 \cdot 2\text{H}_2\text{O} \geq 99\%$) and sodium hydroxide ($\text{NaOH} \geq 99.0\%$) were purchased from Merck. 3-(4,5-Dimethylthiazol-2-yl)-2,5-diphenyltetrazolium bromide (MTT), sodium hypochlorite solution (NaOCl, available chlorine 10–15%), and dimethyl sulfoxide (DMSO) were obtained from Sigma-Aldrich.

Green synthesis of ZnO/CuO NPs. Fresh shoots of *S. nigra* shrub were sterilized with 5% NaOCl and their surface moisture was removed at 25 °C. The plant material was dried with an electric grinder to turned into a soft powder. Then, 7 mL of deionized water was added to 1 g of plant powder, and it was shaken overnight at 25 °C. The prepared mixture was brewed at 100 °C for 10 min. Finally, the plant extract was separated by filter paper and centrifugation. To support the reproducibility, voucher specimens for the described plants

were deposited in University public herbarium. The *S. nigra* Fresh shoots were collected under the licence of the collection of plant or seed specimens in the University in accordance with applicable institutional, national, and international rules and legislation. It was verified by the Iranian Botanical Survey, whose voucher specimen number was 1400/8 deposited at the Department Pharmacognosy, Kerman University.

To synthesize bimetallic NPs, 1.6 g of $\text{Zn}(\text{CH}_3\text{COO})_2$ was added to 100 mL of extracts at 70 °C. After dissolving the zinc salt with a strainer, 0.8 g of CuCl_2 was added to the mixture. The pH of the solution was adjusted to 8 by adding 1 mol/L of NaOH. The mixture was sterilized at 70 °C for 3 h. The ensuing NPs were washed 3 times with deionized water and dried at 90 °C in an oven. Finally, the synthesized NP powder was calcined at 400 °C for 6 h.

Characterization of NPs. XRD analysis was performed with X'PertPro device from Panalytical Holland Company with Anod material Cu (1.54 Å, 40 kV, 30 mA) within a 2θ range of 10° to 80° in order to confirm the expected crystal structure of hexagonal ZnO and monoclinic CuO nanocrystals. The size, surface morphology, and elemental analysis of synthesized NPs were studied by FEG-SEM (microscope Sigma VP; ZEISS, Germany) and EDX analyses (EDX detector from Oxford Instruments Company; UK). The NP analysis at higher magnifications was performed by means of TEM (microscope Tecnai G2 Spirit Twin; FEI, Czech Republic). The TEM microscopy was performed at accelerating voltage of 120 kV and yielded not only standard bright-field images (TEM/BF) of the individual NPs, but also EDX spectra (TEM/EDX; EDX detector from EDAX; USA) and electron diffraction patterns (TEM/SAED; verification of crystalline structure from XRD).

Culturing of cells. Cancer standard cell lines including human melanoma cells A375 and human lung cancer A549 have been prepared from the Pasture Institute Cells Bank, Tehran, Iran. Cancer cells were grown in Dulbecco's Modified Eagles Medium (DMEM) containing 100 IU/mL penicillin and 100 µg/mL streptomycin, 10% Fetal Calf Serum (FCS), 4 mM glutamine and 1 mM sodium pyruvate by incubating at 37 °C in a moistened atmospheric chamber and 5% CO_2 .

Assessment of anticancer activity. The effect of bimetallic NPs was evaluated on the susceptibility of A375 and A549 cell lines using MTT assay. After 24 h of culturing cancer cells in microplates, 100 µL of the ZnO/CuO bimetallic NPs in the concentrations of 1, 10, 100, 500, and 1000 µg/mL were added to each well. Treated plates with ZnO/CuO bimetallic NPs and Doxorubicin with 4 and 8 µg/mL (as positive controls) were incubated at 37 °C and 5% CO_2 for 72 h. Then, 20 µL of MTT solution was added to the treatments and after 4 h of incubation, 100 µL of dimethyl sulfoxide (DMSO) was added to each well. Finally, the absorbance was measured at 490 nm by an enzyme-linked immunosorbent assay (ELISA) reader (BioTeks Elx 800). The survival rate (%) was calculated by the following formula:

$$\text{Survival rate (\%)} = (\text{OD in experimental group} / \text{OD in control group}) \times 100$$

The inhibitory concentration needed for 50% cytotoxicity (IC_{50}) was assessed using the Probit analysis and plotting the level of inhibition *versus* the concentration.

Statistical analysis. All experiments were carried out in triplicate. Data were analyzed using ANOVA followed by unpaired Student's *t*-test. *P*-values of <0.05 were considered statistically significant.

P-values of <0.01 were considered statistically significant.

Ethical statement. We confirm that all methods were carried out under in vitro condition.

Results

Characterization of ZnO/CuO bimetallic NPs. *XRD analysis.* The crystalline structure of the zinc-copper bimetallic NPs calcined at 400 °C is illustrated in Fig. 1. The prominent peaks observed in $2\theta = 32, 34.5, 37, 47.5, 57, 63$ and 69° confirmed the crystalline structure and hexagonal phase of zinc oxide NPs (JCPDS card 01-080-0075). The peaks in the $2\theta = 36, 39, 49, 66.5$ and 68.5° confirmed the crystal structure and monoclinic copper oxide phase (JCPDS card 01-080-1917)⁵⁹. As can be observed in the Fig. 1, the number of clear diffraction and peak intensities of ZnO NPs are higher than of CuO NPs. This indicates that ZnO NPs have higher percentage in the structure of zinc-copper bimetallic NPs and high degree of crystallinity. The peak of low crystallization of CuO NPs is due to the coating role of ZnO NPs on them⁶⁰.

SEM analysis. The surface morphologies, particle sizes and EDX measurements of the bimetallic NPs are shown in Fig. 2. Consequently, Fig. 2a,b depicts that a number of polygonal ZnO NPs⁶¹ are arranged in adjacent spherical NPs. The growth of polygonal shapes of NPs was appropriate in different directions. Figure 2b shows isometric NPs, where size ranged from 20 to 130 nm due to the different shapes of ZnO NPs with CuO. In some portions, the diameter of the prepared ZnO NPs was 98 nm, and also the diameter of some aggregated spherical particles was 130 nm. The presence of Zn, Cu, and O with weight percentages of 59.3, 19.4, and 21.3, respectively, confirmed the high amount of ZnO NPs compared to CuO (Fig. 2c).

TEM analysis. The detailed analysis of ZnO/CuO bimetallic NPs by TEM (Fig. 3) showed the NPs in thin layer deposited on carbon film (TEM/BF; Fig. 3a), confirming their crystalline structures (TEM/SAED; Fig. 3b,c) and their elemental composition (TEM/EDX; Fig. 3d). The TEM/BF micrograph showed that ZnO/CuO bimetal-

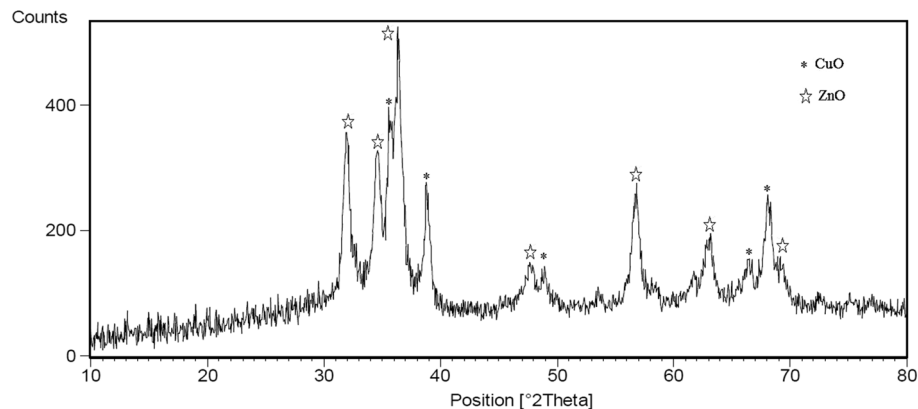


Figure 1. XRD spectrum of the bimetallic ZnO/CuO NPs.

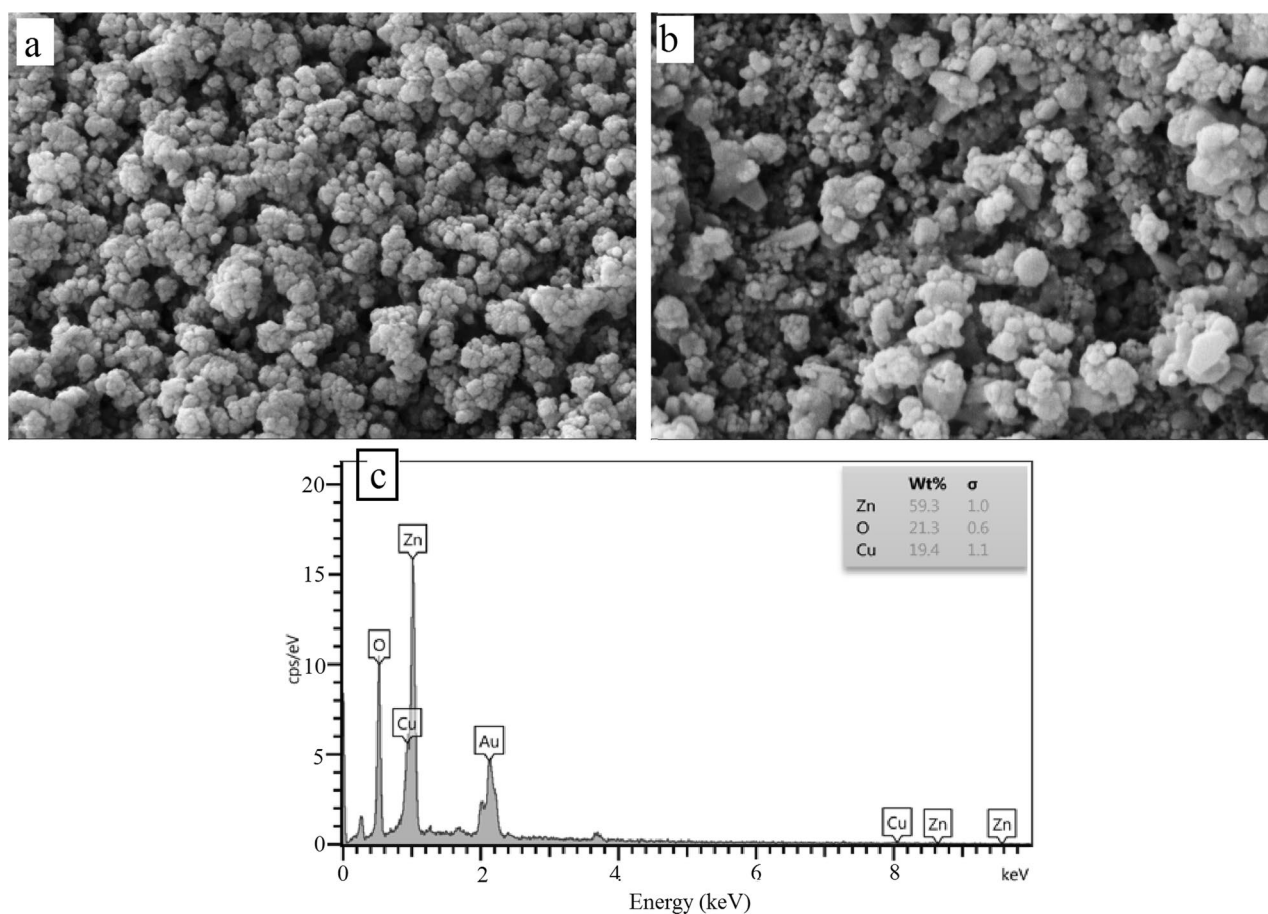


Figure 2. SEM images (a, b) and EDX spectra (c) of the ZnO/CuO NPs.

lic NPs were mostly isometric, tended to form agglomerates during the drying process, and exhibited quite broad particle size distribution (particle diameters from tens to hundreds of nm). The TEM/SAED diffractogram (Fig. 3b) exhibited quite low diffraction intensities. This could be attributed to the fact that relatively low concentration of small particles was deposited on carbon film and the nanoparticle diffractions were hidden in amorphous carbon background. After careful background correction, the comparison of radially averaged TEM/SAED diffraction pattern with theoretically calculated powder XRD of hexagonal ZnO and monoclinic CuO nanocrystals showed quite good agreement (Fig. 3c), confirming the expected crystalline structure. The processing of TEM/SAED patterns and calculation of theoretical power XRD patterns was described in our previous studies^{30,31}. The TEM/EDX spectrum was dominated by peaks of Cu (~11%), Zn (~8%), O (~25%) and C (~37%), while the concentrations of all other elements (Mg, Ca, Cl, Si and P) were below 1%. The high concentration of carbon was due to the fact that the NPs were deposited on the supporting carbon film. The presence of

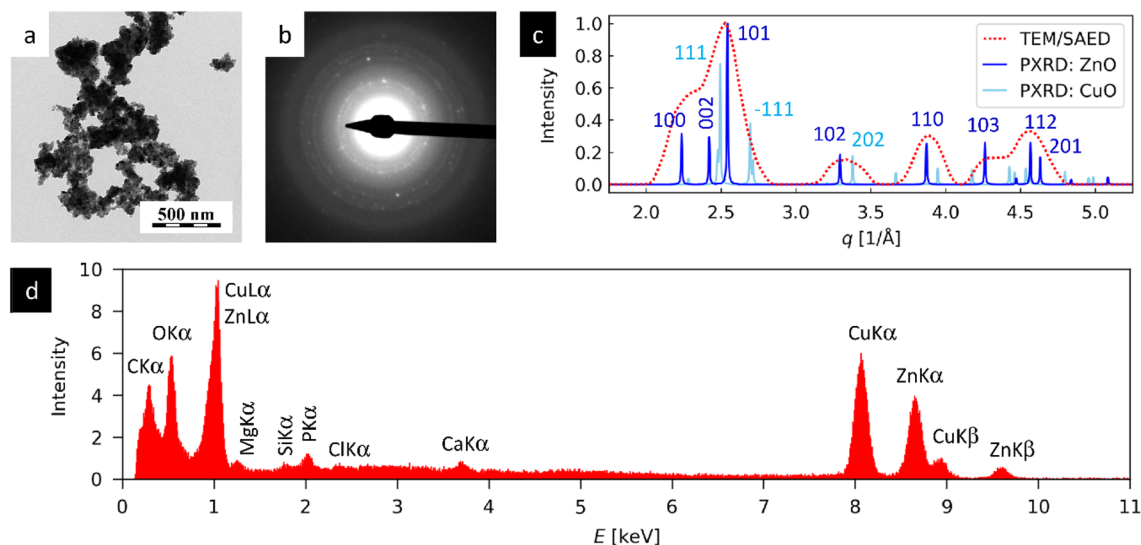


Figure 3. TEM analysis of ZnO/CuO NPs: (a) TEM/BF image demonstrates the morphology of NPs, (b) TEM/SAED diffraction pattern, (c) the comparison of radially averaged experimental TEM/SAED diffractogram with theoretically calculated power XRD diffractograms of ZnO and CuO nanocrystals, and (d) TEM/EDX spectrum of bimetallic ZnO/CuO NPs.

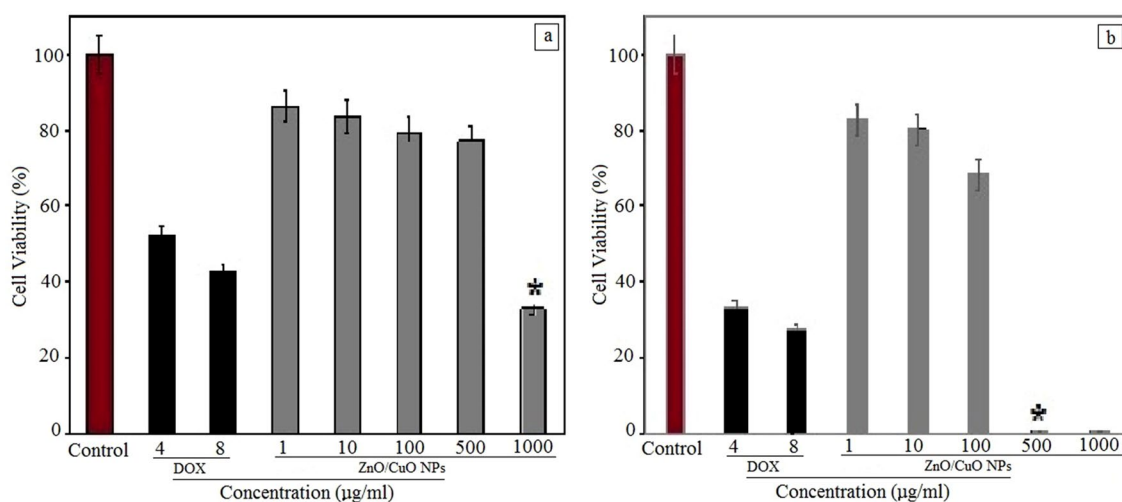


Figure 4. The cell viability (in %) of (a) A549 cell line (Human lung cancer cells) and (b) A375 cell line (human melanoma cancer cells) in the presence of various concentrations of ZnO/CuO NPs, doxorubicin (positive control) and untreated cells (negative control). * $P < 0.01$.

Cu, Zn, and O in approximate ratio 1:1:2 corresponded to the expected composition of ZnO/CuO NPs. The low concentrations of other elements indicated that a small amount of compounds from NP synthesis was remained in the solution and deposited on the carbon film together with the NPs.

Cytotoxicity of the NPs. The in vitro cytotoxic effects of bimetallic ZnO/CuO NPs on A375 and A549 are shown in Fig. 4. The cytotoxicity of untreated cells and doxorubicin (4 and 8 µg/mL) was evaluated as negative and positive control, respectively. The index of anti-proliferative activity of ZnO/CuO bimetallic NPs on A375 cells IC_{50} was 41 µg/mL while this value for A549 cells was 785 µg/mL. Figure 4 shows that these NPs are not very toxic against A549 cancer cells while their toxicity is higher than the evaluated positive control (doxorubicin). These NPs showed remarkable cytotoxic effects towards A375 cancer cells, and at a concentration of 500 µg/mL, the number of cancer cells has reached zero (Fig. 4).

Discussion

The potential therapeutic effects of trace elements against cancers made the metal and metal oxide nanomaterials promising candidates for cancer treatment and diagnosis. Trace elements in the body such as zinc (Zn), copper (Cu), iron, iodine, fluoride, chromium, selenium, manganese and molybdenum are involved in the structure

of metalloenzymes, proteins, immune function DNA production, enzyme function, hormones and antioxidant function. Absorption and accumulation of Cu by cancer cells can cause the angiogenesis of tumors, tumor growth, and proliferation. Since, there is a competition in the uptake of Cu and Zn in cells, the serum levels of them have been evaluated in a variety of cancers^{62,63}. Interestingly, changes in serum levels of Cu to Zn play vital roles in the diagnosis and progression of lung cancer; therefore, the increasing serum Cu levels to Zn has led to the spread of malignant lung tumors⁶². However, serum Cu levels in patients with melanoma are not varied from those in healthy individuals⁶⁴. In this study, the bimetallic ZnO/CuO NPs were successfully synthesized in one-step using *S. nigra* extract. Therefore, we showed the promising potentials of this plant extract for the green, eco-friendly, and cost-effective fabrication of ZnO/CuO NPs. The synthesis of NPs using conventional physico-chemical methods may include the application of expensive devices, materials, toxic/hazardous precursors, high temperatures and pressures, and complicated steps⁶⁰.

The formation of NPs were confirmed by XRD, FEG-SEM, and TEM. The synthesized NPs had hexagonal and monoclinic crystalline structures. The presence of Zn, Cu, and O ions in NPs were verified by EDX analysis. The MTT assay shows the anti-cancer activity of these bimetallic NPs against cancer A549 and A375 cancer cells. Notably, the high toxicity of positive control on A549 cancer cells compared to the prepared ZnO/CuO NPs can be related to the presence of Cu in the synthesized bimetallic ZnO/CuO NPs. However, the bimetallic NPs had a favorable effect on the mortality of A375 cancer cells. According to Zarghami et al.⁶⁵, there was a direct relationship between Cu levels and telomerase gene expression in A549 cancer cells. The enzyme telomerase is active in all cancer cells, and the level of telomerase activity is directly related to the progression of A549 cells. With increase in amount of Cu, the higher activity of this enzyme is occurred, which can result in the development and proliferation of the lung tumors. However, Zn levels do not play a critical role in the progression of this disease⁶⁵. Also, these green-synthesized NPs can be employed for the diagnosis and treatment of other cancer cell lines.

Conclusions

A simple and inexpensive method was established for the green and eco-friendly synthesis of bimetallic ZnO/CuO NPs using *S. nigra* extract as a reducing and stabilizing agent. The high purity of these bimetallic NPs as well as the monoclinic and hexagonal crystalline structures of ZnO and CuO NPs were confirmed by XRD and TEM/SAED diffractograms. The ZnO and CuO NPs with different shapes were existed in the product where the diameter of these NPs ranged approximately from 20 to 130 nm. These bimetallic NPs exhibited low toxicity on A549 cancer cells while their toxicity on A375 cancer cells was dose-dependent and the survival of cancer cells was reduced via an increase in the concentration of the bimetallic NPs. It can be concluded that the serum level of trace elements in different cancer cells is different, and according to the serum level of each element, an appropriate treatment strategy can be deployed for the relevant cancer.

Received: 21 September 2021; Accepted: 24 November 2021

Published online: 06 December 2021

References

- Whiteley, A. E. *et al.* Leukaemia: A model metastatic disease. *Nat. Rev. Cancer* **21**, 461–475 (2021).
- Jamalipour Soufi, G. *et al.* MXenes and MXene-based materials with cancer diagnostic applications: challenges and opportunities. *Comments Inorganic Chem.* **41**(6), 1–34 (2021).
- Selvakumari, D. *et al.* Anti cancer activity of ZnO nanoparticles on MCF7 (breast cancer cell) and A549 (lung cancer cell). *ARPN J. Eng. Appl. Sci.* **10**(12), 5418–5421 (2015).
- Duan, X. *et al.* Zinc oxide nanoparticles synthesized from *Cardiospermum halicacabum* and its anticancer activity in human melanoma cells (A375) through the modulation of apoptosis pathway. *J. Photochem. Photobiol. B Biol.* **202**, 111718 (2020).
- Trayes, K. P. & Cokenakes, S. E. Breast cancer treatment. *Am. Fam. Physician* **104**(2), 171–178 (2021).
- Hamidian, K. *et al.* Doped and un-doped cerium oxide nanoparticles: Biosynthesis, characterization, and cytotoxic study. *Ceramics Int.* **47**(10, Part A), 13895–13902 (2021).
- Haghighat, M. *et al.* Cytotoxicity properties of plant-mediated synthesized K-doped ZnO nanostructures. *Bioprocess Biosyst. Eng.* **45**(1), 1–8 (2022).
- Cheng, Z. *et al.* Nanomaterials for cancer therapy: Current progress and perspectives. *J. Hematol. Oncol.* **14**(1), 1–27 (2021).
- Sartaj, A., Baboota, S. & Ali, J. Assessment of combination approaches of phytoconstituents with chemotherapy for the treatment of breast cancer, a systematic review. *Curr. Pharm. Des.* **27**(45), 4630–4648 (2021).
- Liu, H. *et al.* Detention of copper by sulfur nanoparticles inhibits the proliferation of A375 malignant melanoma and MCF-7 breast cancer cells. *Biochem. Biophys. Res. Commun.* **477**(4), 1031–1037 (2016).
- Mukhtar, M. *et al.* Application of nanotechnology for sensitive detection of low-abundance single-nucleotide variations in genomic DNA: A review. *Nanomaterials* **11**(6), 1384 (2021).
- Barani, M. *et al.* Evaluation of curcumin-loaded niosomes on breast cancer cells: Physicochemical properties, in vitro cytotoxicity, flow cytometric, DNA fragmentation and cell migration assay. *Sci. Rep.* **9**(1), 1–10 (2019).
- Wang, Y. & Wang, F. Post-translational modifications of deubiquitinating enzymes: Expanding the ubiquitin code. *Front. Pharmacol.* **12**, 1434 (2021).
- Sun, S. *et al.* BP4RNaseq: A babysitter package for retrospective and newly generated RNA-seq data analyses using both alignment-based and alignment-free quantification method. *Bioinformatics* **37**(9), 1319–1321 (2021).
- Rahdar, A. *et al.* Biochemical, ameliorative and cytotoxic effects of newly synthesized curcumin microemulsions: Evidence from in vitro and in vivo studies. *Nanomaterials* **11**(3), 817 (2021).
- Torkzadeh-Mahani, M. *et al.* A combined theoretical and experimental study to improve the thermal stability of recombinant D-lactate dehydrogenase immobilized on a novel superparamagnetic Fe₃O₄NPs@metal-organic framework. *Appl. Organometallic Chem.* **34**(5), e5581 (2020).
- Sabir, F. *et al.* DNA based and stimuli-responsive smart nanocarrier for diagnosis and treatment of cancer: Applications and challenges. *Cancers* **13**(14), 3396 (2021).
- Hajizadeh, M. R. *et al.* In vitro cytotoxicity assay of D-limonene niosomes: An efficient nano-carrier for enhancing solubility of plant-extracted agents. *Res. Pharm. Sci.* **14**(5), 448 (2019).

19. Barani, M. *et al.* Lawsone-loaded niosome and its antitumor activity in MCF-7 breast cancer cell line: A nano-herbal treatment for cancer. *DARU J. Pharm. Sci.* **26**, 11–17 (2018).
20. Barani, M. *et al.* Nanodiagnosis and nanotreatment of colorectal cancer: An overview. *J. Nanopart. Res.* **23**(1), 1–25 (2021).
21. Barani, M. *et al.* Nanotreatment and nanodiagnosis of prostate cancer: Recent updates. *Nanomaterials* **10**(9), 1696 (2020).
22. Barani, M. *et al.* Simulation, in vitro, and in vivo cytotoxicity assessments of methotrexate-loaded pH-responsive nanocarriers. *Polymers* **13**(18), 3153 (2021).
23. Barani, M. *et al.* Progress in the application of nanoparticles and graphene as drug carriers and on the diagnosis of brain infections. *Molecules* **26**(1), 186 (2021).
24. Xiao, J.-H. & Zhong, J.-J. Secondary metabolites from Cordyceps species and their antitumor activity studies. *Recent Pat. Biotechnol.* **1**(2), 123–137 (2007).
25. Ji, X. *et al.* Structural characterization of polysaccharide from jujube (*Ziziphus jujuba* Mill.) fruit. *Chem. Biol. Technol. Agric.* **8**(1), 1–7 (2021).
26. Ji, X. *et al.* Metagenomic analysis of gut microbiota modulatory effects of jujube (*Ziziphus jujuba* Mill.) polysaccharides in a colorectal cancer mouse model. *Food Funct.* **11**(1), 163–173 (2020).
27. Pimentel-Moral, S. *et al.* Lipid nanocarriers for the loading of polyphenols—A comprehensive review. *Adv. Colloid Interface. Sci.* **260**, 85–94 (2018).
28. da Volta Soares, M. *et al.* Nanostructured delivery system for zinc phthalocyanine: Preparation, characterization, and phototoxicity study against human lung adenocarcinoma A549 cells. *Int. J. Nanomed.* **6**, 227 (2011).
29. Li, L. *et al.* Simulation of the in vivo fate of polymeric nanoparticles traced by environment-responsive near-infrared dye: A physiologically based pharmacokinetic modelling approach. *Molecules* **26**(5), 1271 (2021).
30. Kostiv, U. *et al.* Monodisperse core-shell NaYF₄:Yb³⁺/Er³⁺@NaYF₄:Nd³⁺-PEG-GGGRGDSGGGY-NH₂ nanoparticles excitable at 808 and 980 nm: Design, surface engineering, and application in life sciences. *Front. Chem.* **8**, 497 (2020).
31. Kostiv, U. *et al.* Physico-chemical characteristics, biocompatibility, and MRI applicability of novel monodisperse PEG-modified magnetic Fe₃O₄&SiO₂ core-shell nanoparticles. *RSC Adv.* **7**(15), 8786–8797 (2017).
32. Cao, Y. *et al.* K-doped ZnO nanostructures: Biosynthesis and parasitocidal application. *J. Mater. Res. Technol.* **15**, 5445–5451 (2021).
33. Sabir, F. *et al.* Nanodiagnosis and nanotreatment of cardiovascular diseases: An overview. *Chemosensors* **9**(4), 67 (2021).
34. Amiri, M. S. *et al.* Plant-based gums and mucilages applications in pharmacology and nanomedicine: A review. *Molecules* **26**(6), 1770 (2021).
35. Alijani, H. Q. *et al.* Biosynthesis of spinel nickel ferrite nanowhiskers and their biomedical applications. *Sci. Rep.* **11**(1), 17431 (2021).
36. Barani, M. *et al.* A new formulation of hydrophobin-coated niosome as a drug carrier to cancer cells. *Mater. Sci. Eng. C* **113**, 110975 (2020).
37. Kouhbanani, M. A. J. *et al.* The inhibitory role of synthesized nickel oxide nanoparticles against Hep-G2, MCF-7, and HT-29 cell lines: The inhibitory role of NiO NPs against Hep-G2, MCF-7, and HT-29 cell lines. *Green Chem. Lett. Rev.* **14**(3), 443–453 (2021).
38. Rahdar, A. *et al.* Deferasirox-loaded pluronic nanomicelles: Synthesis, characterization, in vitro and in vivo studies. *J. Mol. Liq.* **323**, 114605 (2021).
39. Sargazi, S. *et al.* F127/cisplatin microemulsions: In vitro, in vivo and computational studies. *Appl. Sci.* **11**(7), 3006 (2021).
40. Cao, Y. *et al.* Ceramic magnetic ferrite nanoribbons: Eco-friendly synthesis and their antifungal and parasitocidal activity. *Ceramics Int.* **48**, 1–7 (2021).
41. Reshmy, R. *et al.* Nanobiocatalysts: advancements and applications in enzyme technology. *Bioresour. Technol.* **337**, 125491 (2021).
42. Alijani, H. Q. *et al.* Biosynthesis of spinel nickel ferrite nanowhiskers and their biomedical applications. *Sci. Rep.* **11**(1), 1–7 (2021).
43. Rahdar, A. *et al.* Behavioral effects of zinc oxide nanoparticles on the brain of rats. *Inorga. Chem. Commun.* **119**, 1–14 (2020).
44. Khatami, M. *et al.* Waste-grass-mediated green synthesis of silver nanoparticles and evaluation of their anticancer, antifungal and antibacterial activity. *Green Chem. Lett. Rev.* **11**(2), 125–134 (2018).
45. Nazari-Vanani, R. *et al.* A novel self-nanoemulsifying formulation for sunitinib: Evaluation of anticancer efficacy. *Colloids Surf. B Biointerfaces* **160**, 65–72 (2017).
46. Lomeli-Marroquín, D. *et al.* Starch-mediated synthesis of mono- and bimetallic silver/gold nanoparticles as antimicrobial and anticancer agents. *Int. J. Nanomed.* **14**, 2171 (2019).
47. Ghosh, S. *et al.* Novel platinum–palladium bimetallic nanoparticles synthesized by *Dioscorea bulbifera*: Anticancer and antioxidant activities. *Int. J. Nanomed.* **10**, 7477 (2015).
48. Elemike, E. E. *et al.* Green synthesis of Ag, Au and Ag-Au bimetallic nanoparticles using *Stigmaphyllon ovatum* leaf extract and their in vitro anticancer potential. *Mater. Lett.* **243**, 148–152 (2019).
49. Trommschläger, A. *et al.* Gold (i)-BODIPY-imidazole bimetallic complexes as new potential anti-inflammatory and anticancer trackable agents. *Dalton Trans.* **46**(25), 8051–8056 (2017).
50. Sivamaruthi, B. S. *et al.* Biogenic synthesis of silver palladium bimetallic nanoparticles from fruit extract of *Terminalia chebula*—In vitro evaluation of anticancer and antimicrobial activity. *J. Drug Deliv. Sci. Technol.* **51**, 139–151 (2019).
51. Dobrucka, R. *et al.* Evaluation of biologically synthesized Au-CuO and CuO-ZnO nanoparticles against glioma cells and microorganisms. *Saudi Pharm. J.* **27**(3), 373–383 (2019).
52. Elemike, E. E., Onwudiwe, D. C. & Singh, M. Eco-friendly synthesis of copper oxide, zinc oxide and copper oxide–zinc oxide nanocomposites, and their anticancer applications. *J. Inorg. Organomet. Polym. Mater.* **30**(2), 400–409 (2020).
53. Rajeshkumar, S. *et al.* Biosynthesis of zinc oxide nanoparticles using *Mangifera indica* leaves and evaluation of their antioxidant and cytotoxic properties in lung cancer (A549) cells. *Enzyme Microb. Technol.* **117**, 91–95 (2018).
54. Kalaiarasi, A. *et al.* Copper oxide nanoparticles induce anticancer activity in A549 lung cancer cells by inhibition of histone deacetylase. *Biotechnol. Lett.* **40**(2), 249–256 (2018).
55. Chakraborty, R. & Basu, T. Metallic copper nanoparticles induce apoptosis in a human skin melanoma A-375 cell line. *Nanotechnology* **28**(10), 105101 (2017).
56. Hussein, B. Y. & Mohammed, A. M. Green synthesis of ZnO nanoparticles in grape extract: Their application as anti-cancer and anti-bacterial. *Mater. Today Proc.* **42**(3), 18–26 (2021).
57. Ahamed, M. *et al.* Genotoxic potential of copper oxide nanoparticles in human lung epithelial cells. *Biochem. Biophys. Res. Commun.* **396**(2), 578–583 (2010).
58. Mota, A. H. *et al.* Green extraction of *Sambucus nigra* L. for potential application in skin nanocarriers. *Green Mater.* **8**(4), 181–193 (2020).
59. Fang, J. & Xuan, Y. Investigation of optical absorption and photothermal conversion characteristics of binary CuO/ZnO nanofluids. *RSC Adv.* **7**(88), 56023–56033 (2017).
60. Wasim, M. *et al.* Surface modification of bacterial cellulose by copper and zinc oxide sputter coating for UV-resistance/antistatic/antibacterial characteristics. *Coatings* **10**(4), 364 (2020).
61. Khatami, M. *et al.* Rectangular shaped zinc oxide nanoparticles: Green synthesis by Stevia and its biomedical efficiency. *Ceram. Int.* **44**(13), 15596–15602 (2018).
62. Zowczak, M. *et al.* Analysis of serum copper and zinc concentrations in cancer patients. *Biol. Trace Elem. Res.* **82**(1), 1–8 (2001).
63. Soetan, K., Olaiya, C. & Oyewole, O. The importance of mineral elements for humans, domestic animals and plants—A review. *Afr. J. Food Sci.* **4**(5), 200–222 (2010).

64. Ros-Bullon, M., Sanchez-Pedreno, P. & Martinez-Liarte, J. Serum zinc levels are increased in melanoma patients. *Melanoma Res.* **8**(3), 273–277 (1998).
65. Zarghami, N. *et al.* Correlation between serum levels of zinc and copper and telomerase gene expression in lung cancer patients. *Pharma. Sci.* **14**(4), 183–190 (2009).

Acknowledgements

Research reported in this publication was supported by Elite Researcher Grant Committee under award number 4000091 from the National Institute for Medical Research Development (NIMAD), Tehran, Iran (Mehrdad Khatami, Nimad Grant). We also want to thank from Bam University of Medical Sciences, which provided laboratory equipments, and the Slovak Grant Agency VEGA under the contract number 2/0140/20.

Author contributions

All the authors have read and approved the final manuscript. M.K., S.I., S.K., Y.C., H.A.D., M.A.E. and H.A., wrote the main manuscript text and M.S. and H.A. prepared Figs. 2, 3. M.Z., E.B., F.F.D. and M.N. prepared Figs. 1, and 4. All authors reviewed the manuscript.

Competing interests

The authors declare no competing interests.

Additional information

Correspondence and requests for materials should be addressed to M.K. or F.F.D.

Reprints and permissions information is available at www.nature.com/reprints.

Publisher's note Springer Nature remains neutral with regard to jurisdictional claims in published maps and institutional affiliations.



Open Access This article is licensed under a Creative Commons Attribution 4.0 International License, which permits use, sharing, adaptation, distribution and reproduction in any medium or format, as long as you give appropriate credit to the original author(s) and the source, provide a link to the Creative Commons licence, and indicate if changes were made. The images or other third party material in this article are included in the article's Creative Commons licence, unless indicated otherwise in a credit line to the material. If material is not included in the article's Creative Commons licence and your intended use is not permitted by statutory regulation or exceeds the permitted use, you will need to obtain permission directly from the copyright holder. To view a copy of this licence, visit <http://creativecommons.org/licenses/by/4.0/>.

© The Author(s) 2021